Bidirectional amyloid fiber growth for a yeast prion determinant

Thomas Scheibel*‡, Anthony S. Kowal†‡, Jesse D. Bloom† and Susan L. Lindquist*†

The polymerization of many amyloids is a two-stage process initiated by the formation of a seeding nucleus or protofibril. Soluble protein then assembles with these nuclei to form amyloid fibers. Whether fiber growth is bidirectional or unidirectional has been determined for two amyloids. In these cases, bidirectional growth was established by time lapse atomic-force microscopy. Here, we investigated the growth of amyloid fibers formed by NM, the prion-determining region of the yeast protein Sup35p. The conformational changes in NM that lead to amyloid formation in vitro serve as a model for the self-perpetuating conformational changes in Sup35p that allow this protein to serve as an epigenetic element of inheritance in vivo. To assess the directionality of fiber growth, we genetically engineered a mutant of NM so that it contained an accessible cysteine residue that was easily labeled after fiber formation. The mutant protein assembled in vitro with kinetics indistinguishable from those of the wild-type protein and propagated the heritable genetic trait [*PSI*$^+$] with the same fidelity. In reactions nucleated with prelabeled fibers, unlabeled protein assembled at both ends. Thus, NM fiber growth is bidirectional.

Addresses: *Department of Molecular Genetics and Cell Biology and †Howard Hughes Medical Institute, University of Chicago, Chicago, Illinois 60637, USA.
‡These authors contributed equally to this work.

Correspondence: Susan L. Lindquist
E-mail: s-lindquist@uchicago.edu

Received: **18 December 2000**
Revised: **29 January 2001**
Accepted: **30 January 2001**

Published: **6 March 2001**

Current Biology 2001, 11:366–369

0960-9822/01/$ – see front matter

Results and discussion

The [*PSI*$^+$] factor of *S. cerevisiae* is a yeast prion, a protein-based element of inheritance that changes the fidelity of protein translation. The protein determinant of [*PSI*$^+$] is the chromosomally encoded Sup35p, which is required for faithful termination at nonsense codons in messenger RNAs. Sup35p can exist in at least two different stable physical states. The soluble state is associated with accurate translation termination, and the alternate state is associated with a low frequency of nonsense suppression. Once Sup35p acquires its alternate conformation, it influences newly made Sup35p protein to adopt the same state. Therefore, this self-perpetuating change in Sup35p is passed from mother cells to their daughters. Thus, [*PSI*$^+$] represents a new concept in genetics, in which the inheritance of an altered phenotype is due to the propagation of a protein with an altered conformation rather than to an altered nucleic acid [1].

In vitro, the Sup35p prion-determining domain, consisting of the N-terminal (N) and the middle (M) regions, undergoes a conformational change to form amyloid fibers in a process that closely parallels prion propagation in vivo [2, 3]. The rate of fiber formation of purified soluble NM is dramatically increased by the addition of preformed NM fibers. Moreover, the number of "free-nucleating fiber ends" determines the rate of NM fiber assembly [4].

Here, we investigate the directionality of NM amyloid fiber assembly. Previously, atomic force microscopy demonstrated that two other amyloids, synthetic human amylin and β-amyloid, grow in a bidirectional manner [5, 6]. We employed a different method to visualize NM fiber growth. First, we generated a series of NM derivatives in which individual amino acids were changed to cysteine residues. These provided unique sites for the attachment of various probes since NM naturally lacks cysteine (unpublished data). We compared each cysteine-substituted NM mutant (NM^{cys}) with wild-type NM to determine the influence of individual cysteine substitutions on NM structure and fiber assembly in vitro. The kinetics of fiber assembly were monitored by the acquisition of Congo Red binding activity, and fiber morphology was assessed by transmission electron microscopy (TEM) (unpublished data).

Among those mutants that assembled into fibers in a manner indistinguishable from wild-type NM (Figure 1a,b and data not shown), the accessibility of the cysteines after assembly was examined. A cysteine-conjugatable biotin was reacted with NM^{cys} fibers, and the labeling efficiency was determined by the ability of biotinylated protein to compete with a spectroscopically assayable dye for binding to avidin (see Materials and methods). Fibers formed by the mutant, NM^{K184C}, which carried a substitution of cysteine for lysine at residue 184, labeled at a high efficiency, 0.56 ± 0.08 mol (biotin)/mol (monomeric protein).

Figure 1

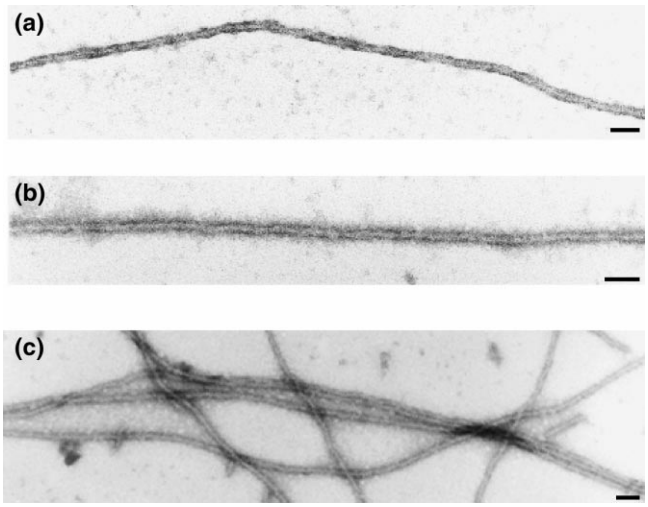

Electron micrographs of NM, NM^{K184C}, and hybrid fibers. **(a)** Micrograph of a negatively stained wild-type NM amyloid fiber. **(b)** The morphology of NM^{K184C} fibers is indistinguishable from that of NM fibers. **(c)** A field view of hybrid fibers formed in a seeded reaction for which sonicated NM^{K184C} fibers were used as nuclei and soluble NM protein was used as source protein. The scale bars represent 50 nm.

Figure 2

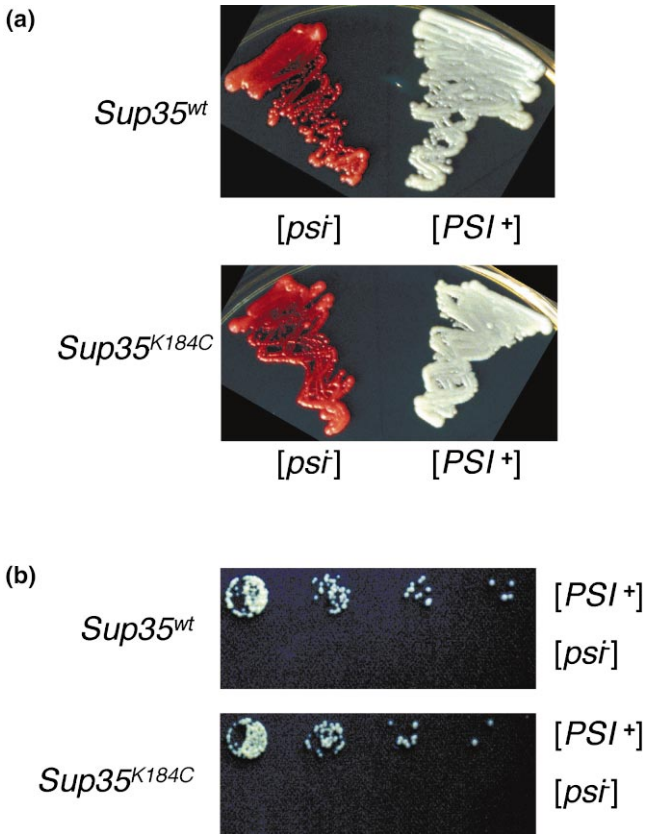

Influence of K184C on the propagation and maintenance of [*PSI*$^+$]. Genomic *Sup35*^{wt} was replaced by *Sup35*^{K184C} in a 74D-694 background, and the mutant strains maintained their ability to support [*psi*$^-$] and [*PSI*$^+$]. **(a)** A comparison between *Sup35*^{wt} and *Sup35*^{K184C} [*psi*$^-$] and [*PSI*$^+$] strains is shown on YPD. White color indicates translation suppression ([*PSI*$^+$]), and red color indicates translation fidelity ([*psi*$^-$]). **(b)** The strains are shown on SD-Ade plates. Five-fold dilutions of 10^6 cells/ml are spotted in each step.

Next, NM^{K184C} fibers were tested for their ability to seed the conformational conversion of soluble wild-type NM in vitro. Preformed NM^{K184C} fibers were sonicated, resulting in an average seed length of 100–500 nm (data not shown). Such seeds nucleated conformational change of soluble wild-type NM with an efficiency similar to that of sonicated wild-type NM fibers and with no difference in fiber assembly rate or fiber morphology (Figure 1c and data not shown).

To ensure that the mutation had not altered the remarkable biological properties of the protein, we used NM^{K184C} to replace the wild-type NM region of the gene encoding Sup35p in the yeast genome (see Materials and methods). When the gene was replaced in a [*psi*$^-$] strain, they remained [*psi*$^-$], while a replaced [*PSI*$^+$] strain remained [*PSI*$^+$] (Figure 2). Moreover, $[psi^-]^{K184C}$ cells exhibited no detectably greater tendency to convert to the [*PSI*$^+$] state than did wild-type strains, and $[PSI^+]^{K184C}$ cells showed no greater tendency to convert to [*psi*$^-$] (Figure 2 and data not shown). Thus, NM^{K184C} has no apparent influence on the conformational conversions that underlie these in vivo phenotypes.

The wild-type behavior of NM^{K184C} and the surface exposure of approximately 50% of its cysteines allowed us to assess the directionality of fiber growth of the prion-determining domain of Sup35p (Figure 3a). After sonication of NM^{K184C} fibers, they were labeled with modified gold colloids in a manner that enabled their visualization by TEM. Monomaleimido Nanogold (Nanoprobes) with a particle diameter of 1.4 nm was covalently cross-linked to the sulfhydryl group of accessible cysteine residues. Electron microscopy confirmed that the gold particles were distributed along the surface of the sonicated NM^{K184C} fibers (Figure 3b). We then employed the gold-labeled fibers to seed fiber growth of soluble wild-type NM protein. The 1.4 nm Nanogold particles were enlarged with Gold-enhance (Nanoprobes), and the resulting mixed fibers were negatively stained for visualization of the fibers and gold particles by TEM. The majority of the fibers contained a short, gold-labeled internal segment, with unlabeled material at both ends (Figure 3c). Occasionally, fibers exhibited gold labeling at one end only (Figure 3c, bottom panel). This might be due to steric hindrance of bound gold particles on fiber ends, or it might reflect occasional improper folding at fiber ends that blocks the addition of new material.

Figure 3

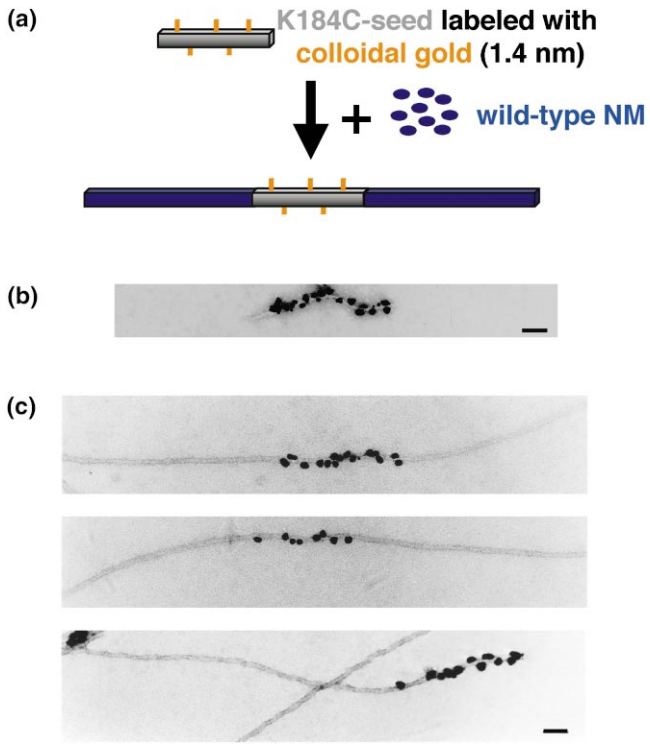

Directionality of NM fiber assembly. **(a)** Sonicated NM^{K184C} fibers were labeled with monomaleimido Nanogold and used to seed fiber assembly of soluble NM. **(b)** Electron micrographs of gold-labeled seeds. Fibers were sonicated prior to gold labeling, and this resulted in an average fiber length from 100 nm to 500 nm. **(c)** Electron micrographs of gold-labeled hybrid fibers. The dense particles are enhanced gold particles attached to the NM^{K184C} nuclei. The top two panels demonstrate the bidirectionality of NM fiber assembly. In some instances, unidirectional fiber assembly can be detected (lower panel). The scale bars represent 50 nm.

Determining the basic parameters of amyloid growth is a critical element in understanding their biological properties. Our results demonstrate that NM fibers, like amylin fibers and β-amyloid fibers, grow bidirectionally in vitro and indicate that they do not have a strong structural polarity. These proteins are unrelated in primary amino acid sequence and have very different biological properties; one is associated with epigenetic inheritance, and the others are associated with a human amyloid disease. Although many more amyloids will need to be tested before these results can be generalized, this observation suggests that bidirectional growth might be a common property of amyloid fiber assembly.

The power of genetic analysis in yeast may make it possible, through genetic screening, to determine if bidirectional growth is a fundamentally important characteristic of amyloid growth. The technique we employed should also provide a general tool for investigating the growth of other amyloid fibers since the method is easily accessible to most laboratories. Moreover, this method provides a general mechanism for the attachment of diverse functional groups to self-assembling protein fibers and for patterning those attachments in defined ways. In combination with different labels, these self-assembling polymers may provide useful materials for producing bio-inspired nano-devices.

Materials and methods

Bacterial strains and culture

Using pEMBL-Sup35p [7] as a template, we amplified DNA encoding NM by PCR with various linkers for subcloning. For recombinant NM expression, the PCR products were subcloned as NdeI–BamHI fragments into pJC25 [8]. For site-directed mutagenesis, the protocol by Howorka and Bayley [9] was used for a high-throughput cysteine scanning mutagenesis. A nonmutagenic primer pair for the β-lactamase gene and a mutagenic primer pair for each respective mutant were employed. In addition to generating a unique NsiI site, as in the original protocol, we used SphI and NspI sites (allows introduction of a cysteine codon in front of methionine and isoleucine or after the alanine and threonine codons) to increase the number of mutants in our cysteine screen. Each construct was confirmed by Sanger sequencing. Proteins were expressed in *E. coli* BL21 [DE3] upon induction with 1 mM IPTG (OD_{600nm} of 0.6) at 25°C for 3 hr.

Protein purification

We purified NM after recombinant expression in *E. coli* by chromatography by using Q-Sepharose (Pharmacia), hydroxyapatite (BioRad), and Poros HQ (Boehringer Mannheim) as a final step. All purification steps for NM were performed in the presence of 8 M urea. Protein concentrations were determined with the calculated extinction coefficient of 0.90 for a 1 mg/ml NM solution in a 1 cm cuvette at 280 nm [10].

Yeast strains and culture

Using pJC25NM^{K184C} as a template, we amplified DNA by PCR with two EcoRI sites for subcloning, subcloned it into the integrative construct pJLI-Sup35pC [PSI^+] [3], and confirmed its fidelity by Sanger sequencing. To investigate the propagation and maintenance of [PSI^+] of $Sup35^{K184C}$, we used MluI for the digestion of the integrative construct and transformed the construct into 74-D694 [PSI^+] and [psi^-] strains. Transformants were selected on uracil-deficient (SD-Ura) medium, and recombinant excision events were selected on medium containing 5-fluoroorotic acid. The resulting strains were confirmed by genomic PCR, followed by digestion with NspI for the new restriction site. Strains were tested for the presence of [PSI^+] by spotting on rich media (YPD) and synthetic media lacking adenine (SD-Ade), and they were checked for prion-curing on YPD plates with 5 mM guanidinium hydrochloride, as described previously [11, 12].

Biotinylation of NM^{K184C} fibers

EZ-link PEO-maleimide–conjugated biotin (Pierce) was covalently linked to the assembled NM^{K184C} fibers for 2 hr at 25°C according to the manufacturer's protocol. Remaining free biotin was removed by size exclusion chromatography with D-Salt Excellulose desalting columns (Pierce). We determined labeling efficiency by examining the competition between biotin and [2-(4′-hydroxybenzene)] benzoic acid (HABA) for avidin binding. The binding of HABA to avidin results in a specific absorption band at 500 nm, which is decreased proportionately when biotin is added since biotin displaces the dye due to its higher affinity for avidin [13].

Gold labeling of NM^{K184C} fibers

NM^{K184C} fibers were sonicated for 15 s in order to gain short fibers for efficient seeding [4]. Monomaleimido Nanogold (Nanoprobes) with a particle diameter of 1.4 nm was covalently cross-linked to assembled

sonicated NM^{K184C} fibers for 18 hr at 4°C according to the manufacturer's protocol. Remaining free Nanogold was removed by size exclusion chromatography with D-Salt Excellulose desalting columns (Pierce). The extent of labeling was determined by UV/visible absorption with extinction coefficients for Nanogold of 2.25×10^5 at 280 nm and 1.12×10^5 at 420 nm. Ratios of optical densities at 280 nm and 420 nm allowed an approximation of the labeling efficiency. Soluble wild-type NM was seeded with gold-labeled NM^{K184C}, and fiber growth was allowed to occur at room temperature for 1 hr.

Electron microscopy

In order to visualize the 1.4 nm Nanogold particles, we employed an "on-grid" enhancement of the gold particles with Goldenhance (Nanoprobes). Equal volumes of enhancer and activator were mixed and incubated for 15 min at room temperature. The addition of an equal volume of initiator and dilution (1:2) with phosphate buffer revealed the final enhancing reagent. Six microliter protein (8 μM, 1% or 2% (w/w) gold-labeled sonicated seed) was applied to a 400 mesh carbon-coated copper grid (Ted Pella) for 45 s. After the grids were washed with 100 μl phosphate buffer, they were incubated, sample side down, on a drop of Goldenhance reagent for 5 min. After the grids were washed with 200 μl glass-distilled water, negative staining with 2% aqueous uranyl acetate was employed as previously described [14]. Images were obtained with a Philips CM120 transmission electron microscope with an LaB_6 filament, operating at 120 kV in low-dose mode at a magnification of 45,000 × and recorded on Kodak SO163 film.

Acknowledgements

This research was supported by the Kemper Foundation (T. S.), a postdoctoral fellowship (SCHE 603/1-1) of the Deutsche Forschungsgemeinschaft (T. S.), the Keck Foundation, the University of Chicago Materials Research Science and Engineering Center, the National Institutes of Health, and the Howard Hughes Medical Institute. J. B. was supported by a grant for undergraduate education from the Howard Hughes Medical Institute.

References

1. Serio TR, Lindquist S: **[PSI+]: an epigenetic modulator of translation termination efficiency.** *Annu Rev Cell Dev Biol* 1999, **15:**661-703.
2. Glover JR, Kowal AS, Schirmer EC, Patino MM, Liu JJ, Lindquist S: **Self-seeded fibers formed by Sup35, the protein determinant of [PSI+], a heritable prion-like factor of S. cerevisiae.** *Cell* 1997, **89:**811-819.
3. Liu JJ, Lindquist S: **Oligopeptide-repeat expansions modulate 'protein-only' inheritance in yeast.** *Nature* 1999**, 400:**573-576.
4. Serio TR, Cashikar AG, Kowal AS, Sawicki GJ, Moslehi JJ, Serpell L, *et. al.*: **Nucleated conformational conversion and the replication of conformational information by a prion determinant.** *Science* 2000, **289:**1317-1321.
5. Goldsbury C, Kistler J, Aebi U, Arvinte T, Cooper GJS: **Watching amyloid fibrils grow by time-lapse atomic force microscopy**. *J Mol Biol* 1999, **285:**33-39.
6. Blakley HK, Sanders GH, Davies MC, Roberts CJ, Tendler SJ, Wilkinson MJ: **In-situ atomic force microscopy study of β-amyloid fibrillization.** *J Mol Biol* 2000, **298:**833-840.
7. Ter-Avanesyan MD, Kushnirov VV, Dagkesamanskaya AR, Didichenko SA, Chernoff YO, Inge-Vechtomov SG, *et al.*: **Deletion analysis of the Sup35p gene of the yeast Saccharomyces cerevisiae reveals two non-overlapping functional regions in the encoded protein.** *Mol Microbiol* 1993, **7:**683-692.
8. Clos J, Brandau S: **pJC20 and pJC40-two high-copy-number vectors for T7 RNA polymerase-dependent expression of recombinant genes in Escherichia coli.** *Protein Expr Purif* 1994, **5:**133-137.
9. Howorka S, Bayley H: **Improved protocol for high-throughput cysteine scanning mutagenesis.** *Biotechniques* 1998, **25:**764-766.
10. Gill SC, von Hippel PH: **Calculation of protein extinction coefficients from amino acid sequence data.** *Anal Biochem* 1989, **182:**319-326.
11. Tuite MF, Mundy CR, Cox BS: **Agents that cause a high frequency of genetic change from [PSI+] to [psi-] in Saccharomyces cerevisiae.** *Genetics* 1981, **98:**691-711.
12. Derkatch IL, Chernoff YO, Kushnirov VV, Inge-Vechtomov SG, Liebman SW: **Genesis and variability of [PSI] prion factors in Saccharomyces cerevisiae.** *Genetics* 1996, **144:**1375-1386.
13. Green NM: **A spectrophotometric assay for avidin and biotin based on binding of dyes by avidin.** *Biochem J* 1965, **94:**23c-24c.
14. Spiess E, Zimmermann HP, Lunsdorf H: **Negative staining of protein molecules and filaments.** In *Electron Microscopy in Molecular Biology – A Practical Approach.* Edited by Sommerville J, Scheer U. Oxford: IRL Press Ltd.; 1987:147-166.